Commun Nonlinear Sci Numer Simulat 83 (2020) 105135

Contents lists available at ScienceDirect

Commun Nonlinear Sci Numer Simulat

journal homepage: www.elsevier.com/locate/cnsns

Research paper

Bäcklund transformation, exact solutions and interaction behaviour of the (3+1)-dimensional Hirota-Satsuma-Ito-like equation

Si-Jia Chen[a], Wen-Xiu Ma[b,c,d,e,f,g], Xing Lü[a,*]

[a] Department of Mathematics, Beijing Jiao Tong University, Beijing 100044, China
[b] Department of Mathematics, Zhejiang Normal University, Jinhua 321004, Zhejiang, China
[c] Department of Mathematics, King Abdulaziz University, Jeddah, Saudi Arabia
[d] School of Mathematics, South China University of Technology, Guangzhou 510640, China
[e] Department of Mathematics and Statistics, University of South Florida, Tampa, FL 33620, USA
[f] College of Mathematics and Systems Science, Shandong University of Science and Technology, Qingdao 266590, Shandong, China
[g] International Institute for Symmetry Analysis and Mathematical Modelling, Department of Mathematical Sciences, North-West University, Mafikeng Campus, Private Bag X 2046, Mmabatho 2735, South Africa

A R T I C L E I N F O

Article history:
Received 6 July 2019
Revised 2 November 2019
Accepted 23 November 2019
Available online 25 November 2019

MSC:
35A25
37K10

Keywords:
Hirota bilinear form
Bäcklund transformation
Lump solutions
Interaction phenomena

A B S T R A C T

In this paper, a (3+1)-dimensional Hirota-Satsuma-Ito-like equation is introduced based on the (2+1)-dimensional Hirota-Satsuma-Ito equation. Bäcklund transformation and corresponding exponential function solutions are deduced by virtue of the Hirota bilinear form. The lump solutions are constructed and the interaction phenomena between a lump wave and multi-kink waves are discussed. The lump wave may turn up in different positions and can be swallowed by multi-kink waves, which means that the collision is non-elastic. Finally, the dynamical behavior of the interaction phenomena is numerically simulated.

1. Introduction

Nonlinear evolution equations (NLEEs) play a crucial role in the areas of physics, chaos and engineering [1–6]. Searching for exact solutions to NLEEs is of value and significance in the study of nonlinear dynamics [7–16]. Bäcklund transformations (BTs) relate two solutions of same equations or different equations. Transformations between two different solutions of an equation are generally called auto-BTs [17,18]. BTs have many forms, including bilinear form, Bell polynomials form, Wahlquist-Estabrook form and Painlevé form [19–25]. Many NLEEs have BTs, such as the Kuramoto-Sivashinsky equation [26], the Kadomtsev-Petviashvili equation [27], a (3+1)-dimensional generalized KP equation [28], the (3+1)-dimensional BKP equation [29]. The test function method combining many types of functions provides an approach for constructing exact solutions to NLEEs. In Ref. [30], based on positive quadratic function solutions to a bilinear equation, lump solutions

* Corresponding author.
E-mail addresses: wma3@usf.edu (W.-X. Ma), xlv@bjtu.edu.cn (X. Lü).

https://doi.org/10.1016/j.cnsns.2019.105135

to the Kadomtsev-Petviashvili equation have been derived with symbolic computation. In Ref. [31], based on a rational-cosh-cos type test function, the interaction phenomena among the lump waves, kink waves and periodic waves to the (3+1)-dimensional Jimbo-Miwa equation have been studied.

Lump solutions, as a kind of rational solutions, are real, nonsingular, and algebraically decay in all directions [32–38]. Lump solutions can be widely used to describe the rogue wave in Bose-Einstein condensate [39], the freak wave in the ocean [40] and the nonlinear localized wave in plasma [41]. Recently, with the development of nonlinear dynamics, abundant interaction solutions between the lump and other solutions have attracted much attention, such as lump-kink and lump-soliton solutions [42–47].

The Hirota-Satsuma (HS) equation

$$u_t - u_{xxt} - 3uu_t + 3u_x \int_x^{\infty} u_t dx + u_x = 0, \tag{1}$$

with $u = u(x, t)$ is firstly proposed by Hirota and Satsuma as a model equation describing the unidirectional propagation of shallow water waves [48]. The dependent variable transformation $u(x, t) = 2(\ln f(x, t))_{xx}$ yields the Hirota bilinear form of Eq. (1)

$$(D_x D_t - D_x^3 D_t + D_x^2) f \cdot f = 0. \tag{2}$$

The differential operator D [19] is defined by

$$D_x^{n_1} D_y^{n_2} D_z^{n_3} D_t^{n_4} (f \cdot g) = \left(\frac{\partial}{\partial x} - \frac{\partial}{\partial x'}\right)^{n_1} \left(\frac{\partial}{\partial y} - \frac{\partial}{\partial y'}\right)^{n_2} \left(\frac{\partial}{\partial z} - \frac{\partial}{\partial z'}\right)^{n_3} \left(\frac{\partial}{\partial t} - \frac{\partial}{\partial t'}\right)^{n_4} f(x, y, z, t) g(x', y', z', t')\Big|_{x'=x, y'=y, z'=z, t'=t},$$

where n_1, n_2, n_3, n_4 are nonnegative integers, while $f(x, y, z, t)$ and $g(x, y, z, t)$ are two functions.

The Hirota-Satsuma-Ito (HSI) equation [49]

$$w_t - u_{xxt} - 3uu_t + 3u_x v_t - \alpha u_x = 0, \quad w_x = -u_y, \quad v_x = -u, \tag{3}$$

enjoying the Hirota bilinear form

$$(D_x^3 D_t + D_y D_t + \alpha D_x^2) f \cdot f = 0, \tag{4}$$

is an integrable (2+1)-dimensional extension of Eq. (1), where α is a real nonzero constant and $u(x, y, t) = 2(\ln f(x, y, t))_{xx}$.

We extend the (2+1)-dimensional HSI equation into the following (3+1)-dimensional form

$$\alpha w_t - p_{xxt} - 3pp_t + 3p_x v_t - \beta q_t = 0, \quad w_x = -p_y, \quad v_x = -p, \quad q_x = p_z, \tag{5}$$

where β is a real nonzero constant. Setting $p = u_x$ in Eq. (5), we can obtain the (3+1)-dimensional Hirota-Satsuma-Ito-like (HSIl) equation

$$\alpha w_t - u_{xxxt} - 3u_x u_{xt} + 3u_{xx} v_t - \beta q_t = 0, \quad w_x = -u_{xy}, \quad v_x = -u_x, \quad q_x = u_{xz}, \tag{6}$$

and its Hirota bilinear form

$$(D_x^3 D_t + \alpha D_y D_t + \beta D_z D_t) f \cdot f = 0, \tag{7}$$

under the transformation $u(x, y, z, t) = 2(\ln f(x, y, z, t))_x$. The (3+1)-dimensional HSIl equation is a new nonlinear wave model. Different from the previous research, we combine rational functions with multi-cosh functions to construct a new test function. Furthermore, assigning values to some variables, we directly obtain interaction solutions with symbolic computation. The various interaction phenomena provide powerful support for the study of dynamical behavior of the nonlinear waves.

The paper is organized as follows. Bäcklund transformation of the (3+1)-dimensional HSIl equation will be obtained. Exponential function solutions will be derived by applying the corresponding bilinear Bäcklund transformation in Section 2. The interaction phenomena between the lump and multi-kink waves will be studied based on the rational-multi-exp and rational-multi-cosh type test functions in Section 3 and Section 4, respectively. Finally, some conclusions will be given in Section 5.

2. Bilinear Bäcklund transformation

We assume that the bilinear (3+1)-dimensional HSIl equation has another solution g

$$(D_x^3 D_t + \alpha D_y D_t + \beta D_z D_t) g \cdot g = 0, \tag{8}$$

and consider the following form

$$P = [(D_x^3 D_t + \alpha D_y D_t + \beta D_z D_t) g \cdot g] f^2 - g^2 [(D_x^3 D_t + \alpha D_y D_t + \beta D_z D_t) f \cdot f]. \tag{9}$$

Using the exchange identities for the Hirota bilinear operators [19]:

$$[D_x D_t a \cdot a] b^2 - a^2 [D_x D_t b \cdot b] = 2 D_x (D_t a \cdot b) \cdot ba, \tag{10}$$

$$
\begin{aligned}
[D_x^3 D_y a\cdot a]b^2 - a^2[D_x^3 D_y b\cdot b] = {} & 3D_y(D_x a\cdot b)\cdot(D_x^2 a\cdot b) - D_y(D_x^3 a\cdot b)\cdot ab \\
& +3D_x[(D_x^2 D_y a\cdot b)\cdot ab + (D_y a\cdot b)\cdot(D_x^2 a\cdot b)],
\end{aligned}
\tag{11}
$$

we transform Eq. (9) into the following form

$$
\begin{aligned}
P &= [(D_x^3 D_t + \alpha D_y D_t + \beta D_z D_t)g\cdot g]f^2 - g^2[(D_x^3 D_t + \alpha D_y D_t + \beta D_z D_t)f\cdot f] \\
&= [(D_x^3 D_t g\cdot g)f^2 - g^2(D_x^3 D_t f\cdot f)] + [(\alpha D_y D_t g\cdot g)f^2 - g^2(\alpha D_y D_t f\cdot f)] + [(\beta D_z D_t g\cdot g)f^2 - g^2(\beta D_z D_t f\cdot f)] \\
&= 3D_t(D_x g\cdot f)\cdot(D_x^2 g\cdot f) - D_t(D_x^3 g\cdot f)\cdot gf + 3D_x[(D_x^2 D_t g\cdot f)\cdot gf + (D_t g\cdot f)\cdot(D_x^2 g\cdot f)] \\
&\quad + 2\alpha D_t(D_y g\cdot f)\cdot gf + 2\beta D_t(D_z g\cdot f)\cdot gf \\
&= 3D_t(D_x g\cdot f)\cdot[(D_x^2 + \lambda_1 D_x)g\cdot f] + 3D_x(D_t g\cdot f)\cdot[(D_x^2 + \lambda_2 D_t)g\cdot f] \\
&\quad + D_t[(-D_x^3 + 2\alpha D_y + 3\lambda_3\lambda_6 D_y + 2\beta D_z)g\cdot f]\cdot gf + 3D_x[(D_x^2 D_t + \lambda_3 D_y + \lambda_4 D_z)g\cdot f]\cdot gf \\
&\quad - 3\lambda_3 D_y[(D_x + \lambda_5 D_z + \lambda_6 D_t)g\cdot f]\cdot gf + D_z[(-3\lambda_4 D_x + 3\lambda_3\lambda_5 D_y)g\cdot f]\cdot gf,
\end{aligned}
\tag{12}
$$

where $\lambda_i (1 \le i \le 6)$ are arbitrary constants.

Therefore, the decoupling of Eq. (12) gives rise to an alternative BT for Eq. (7) as

$$
\begin{cases}
(D_x^2 + \lambda_1 D_x)g\cdot f = 0, \\
(D_x^2 + \lambda_2 D_t)g\cdot f = 0, \\
(-D_x^3 + 2\alpha D_y + 3\lambda_3\lambda_6 D_y + 2\beta D_z)g\cdot f = 0, \\
(D_x^2 D_t + \lambda_3 D_y + \lambda_4 D_z)g\cdot f = 0, \\
(D_x + \lambda_5 D_z + \lambda_6 D_t)g\cdot f = 0, \\
(-3\lambda_4 D_x + 3\lambda_3\lambda_5 D_y)g\cdot f = 0.
\end{cases}
\tag{13}
$$

We choose $f = 1$ as a solution to the bilinear (3+1)-dimensional HSII equation, which corresponds to the solution $u = 2(\ln f)_x = 0$ to the (3+1)-dimensional HSII equation. Solving Eq. (13), we have

$$
\begin{cases}
g_{xx} + \lambda_1 g_x = 0, \\
g_{xx} + \lambda_2 g_t = 0, \\
-g_{xxx} + 2\alpha g_y + 3\lambda_3\lambda_6 g_y + 2\beta g_z = 0, \\
g_{xxt} + \lambda_3 g_y + \lambda_4 g_z = 0, \\
g_x + \lambda_5 g_z + \lambda_6 g_t = 0, \\
-3\lambda_4 g_x + 3\lambda_3\lambda_5 g_y = 0.
\end{cases}
\tag{14}
$$

We consider a class of exponential function solutions by taking $g = 1 + \varepsilon e^{kx+ly+mz-wt}$, where ε, k, l, m and w are all constants to be determined.

A direct computation with Maple tells

$$
\left\{ k = -\lambda_5 m + \lambda_6 w,\ l = -\frac{p_1}{\alpha},\ \lambda_1 = \lambda_5 m - \lambda_6 w,\ \lambda_2 = \frac{p_2}{w},\ \lambda_3 = \frac{(-p_1 + \beta m)\alpha}{p_1\lambda_6},\ \lambda_4 = \frac{\lambda_5 p_2}{\lambda_6} \right\},
$$

where

$$
p_1 = -\lambda_5^3 m^3 + 3\lambda_5^2\lambda_6 m^2 w - 3\lambda_5\lambda_6^2 m w^2 + \lambda_6^3 w^3 + \beta m, \qquad p_2 = \lambda_5^2 m^2 - 2\lambda_5\lambda_6 m w + \lambda_6^2 w^2.
$$

Therefore, the corresponding exponential function solution to Eq. (7) is as follows

$$
g = 1 + \varepsilon e^{(-\lambda_5 m + \lambda_6 w)x - \frac{p_1}{\alpha}y + mz - wt},
\tag{15}
$$

and

$$
u = 2(\ln g(x,y,z,t))_x = \frac{2\varepsilon(-\lambda_5 m + \lambda_6 w)e^{(-\lambda_5 m + \lambda_6 w)x - \frac{p_1}{\alpha}y + mz - wt}}{1 + \varepsilon e^{(-\lambda_5 m + \lambda_6 w)x - \frac{p_1}{\alpha}y + mz - wt}},
\tag{16}
$$

solves the (3+1)-dimensional HSII equation.

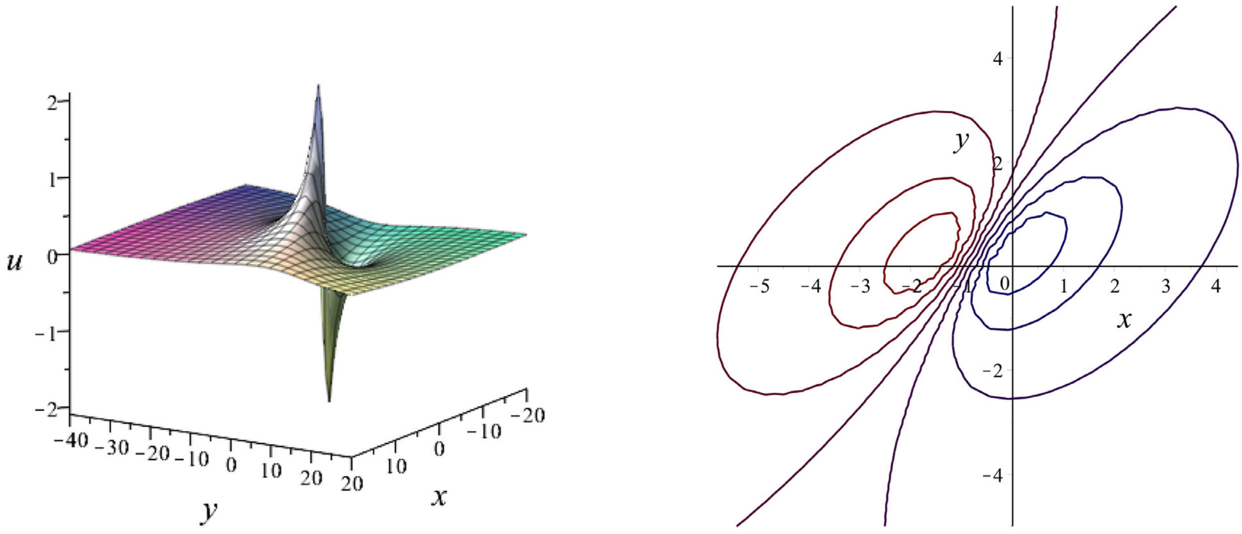

(a) (b)

Fig. 1. Plots of the lump solution with $t = 0$ and $z = 1$: (a) 3-dimensional plot; (b) contour plot.

3. Interaction phenomena between a lump wave and a kink wave

We consider the following test function which is a combination of a positive quadratic function and exponential functions

$$f = m^2 + n^2 + k_9 e^{k_1 x + k_2 y + k_3 z + k_4 t} + k_{10} e^{k_5 x + k_6 y + k_7 z + k_8 t} + k_{11} e^{k_1 x + k_2 y + k_3 z + k_4 t} e^{k_5 x + k_6 y + k_7 z + k_8 t} + c, \tag{17}$$

where

$$m = a_1 x + a_2 y + a_3 z + a_4 t + a_5,$$

$$n = a_6 x + a_7 y + a_8 z + a_9 t + a_{10},$$

while $a_i\,(1 \le i \le 10), k_j\,(1 \le j \le 11)$ and c are all constants.

Case 1

When the parameters satisfy $k_9 = k_{10} = k_{11} = 0$, f reduces to a positive quadratic function, the corresponding $u = 2(\ln f)_x$ degenerates into the lump solution. Substituting Eq. (17) into Eq. (7), and setting all the coefficients of x, y, z, t to zero, we obtain the following relations of parameters

$$\left\{ a_1 = -\frac{a_6 a_9}{a_4},\ a_3 = -\frac{\alpha a_2}{\beta},\ a_8 = -\frac{\alpha a_7}{\beta} \right\},$$

which need to satisfy $a_4 \beta \neq 0$.

We take a selection of the parameters $\alpha = 1,\ \beta = 2,\ a_2 = 2,\ a_4 = 1,\ a_5 = -1,\ a_6 = 1,\ a_7 = 1,\ a_9 = 2,\ a_{10} = 1$ and $a_{11} = 3$ to plot the lump solution in Fig. 1. The corresponding solution to the bilinear (3+1)-dimensional HSII equation is

$$f = (t - 2x + 2y - z - 1)^2 + \left(2t + x + y - \frac{1}{2}z + 1\right)^2 + 3, \tag{18}$$

which yields the lump solution to the (3+1)-dimensional HSII equation

$$u = 2(\ln f(x, y, z, t))_x = \frac{2(10x - 6y + 3z + 6)}{(t - 2x + 2y - z - 1)^2 + (2t + x + y - \frac{1}{2}z + 1)^2 + 3}. \tag{19}$$

Case 2

When the parameters satisfy $k_9 = k_{11} = 0$ or $k_{10} = k_{11} = 0$, $u = 2(\ln f)_x$ degenerates into the interaction solution between a lump wave and a kink wave. When $k_9 = k_{11} = 0$, we consider the case of $a_4 = 1$. With symbolic computation, we obtain relations of the parameters

$$\left\{ a_1 = -a_9 a_6,\ a_3 = -\frac{a_2 \alpha}{\beta},\ a_8 = -\frac{\alpha a_7}{\beta},\ k_7 = -\frac{k_5^3 + \alpha k_6}{\beta},\ k_8 = 0 \right\},$$

which need to satisfy $\beta \neq 0$.

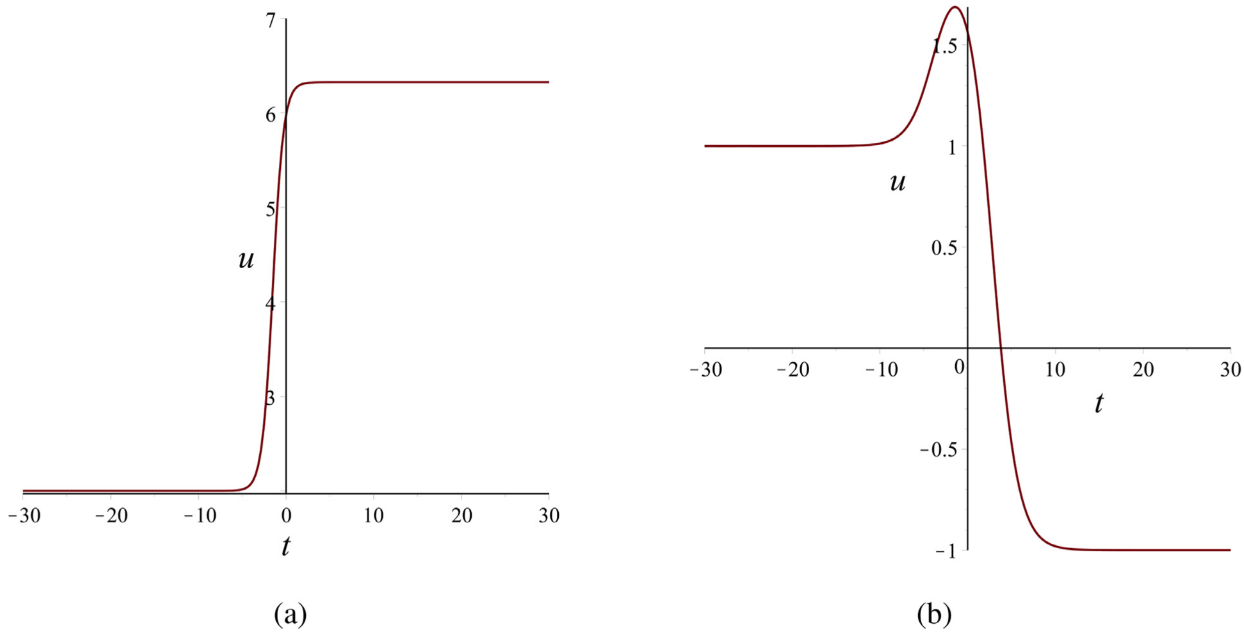

Fig. 2. (a) The plot of u in Eq. (23). (b) The plot of u in Eq. (30).

For a special set of parameters $\alpha = 1,\ \beta = 2,\ c = 2,\ a_2 = 2,\ a_5 = 1,\ a_6 = 2,\ a_7 = 1,\ a_9 = 2,\ a_{10} = 1,\ k_5 = 1,\ k_6 = 1$ and $k_{10} = 1$, we have

$$f = (-4x + 2y - z + t + 1)^2 + \left(2x + y - \frac{1}{2}z + 2t + 1\right)^2 + e^{x+y-z} + 2, \tag{20}$$

and

$$u = 2(\ln f(x,y,z,t))_x = \frac{2(-4 + e^{x+y-z} + 40x - 12y + 6z)}{(-4x + 2y - z + t + 1)^2 + (2x + y - \frac{1}{2}z + 2t + 1)^2 + e^{x+y-z} + 2}. \tag{21}$$

For further simulating the propagation of the lump wave, we select

$$f_1 = (-4x + 2y + t)^2 + \left(2x + y + \frac{1}{2} + 2t\right)^2 + 2. \tag{22}$$

Substituting the extreme point of $u_1 = 2(\ln f_1(x,y,t))_x$ into Eq. (21) with $z = 1$, we have

$$u = \frac{2(e^{-\frac{13}{8}t - \frac{11}{8} + \frac{\sqrt{10}}{10}} + 4\sqrt{10})}{4 + e^{-\frac{13}{8}t - \frac{11}{8} + \frac{\sqrt{10}}{10}}}, \tag{23}$$

which represents the amplitude of the extreme point of u_1.

The lump wave generates from the kink wave and then separates from it (see Fig. 3). With the increase of the time t, the amplitude of the kink wave remains constant. By observing the change of u in Eq. (23), we can find that the lump wave always exists when $t \to +\infty$ and its amplitude remains constant (see Fig. 2(a)).

Case 3

When the parameters satisfy $k_9 k_{10} k_{11} \neq 0$, $u = 2(\ln f)_x$ degenerates into the interaction solution between a lump wave and a kink wave. Substituting Eq. (17) into Eq. (7), and setting all the coefficients of x, y, z, t to zero with $k_9 = 2,\ k_{10} = 1$ and $k_{11} = 1$, we obtain the relations of the parameters in Appendix A. A selection of parameters $\alpha = \frac{1}{2},\ \beta = -1,\ c = -9,\ a_2 = -20,\ a_4 = 10,\ a_6 = 2,\ a_7 = 20,\ a_9 = 34,\ a_{10} = 0,\ k_1 = 1,\ k_2 = 2$ and $k_6 = -4$ of the first case in Appendix A leads to

$$f = \left(-\frac{34}{5}x - 20y - 10z + 10t\right)^2 + (2x + 20y + 10z + 34t)^2 - 9 + e^{x-2y} + 2e^{x+2y+2z} + e^{-4y-2z}, \tag{24}$$

and

$$u = 2(\ln f(x,y,z,t))_x = \frac{2(e^{x-2y} + 2e^{x+2y+2z} + \frac{2512}{25}x + 352y + 176z)}{f}. \tag{25}$$

The fusion process showed in Fig. 4 is different from the fission process in Fig. 3. The lump wave generates and gradually approaches the turning point of the kink wave. Finally, the lump wave is swallowed by the kink wave (see Fig. 4).

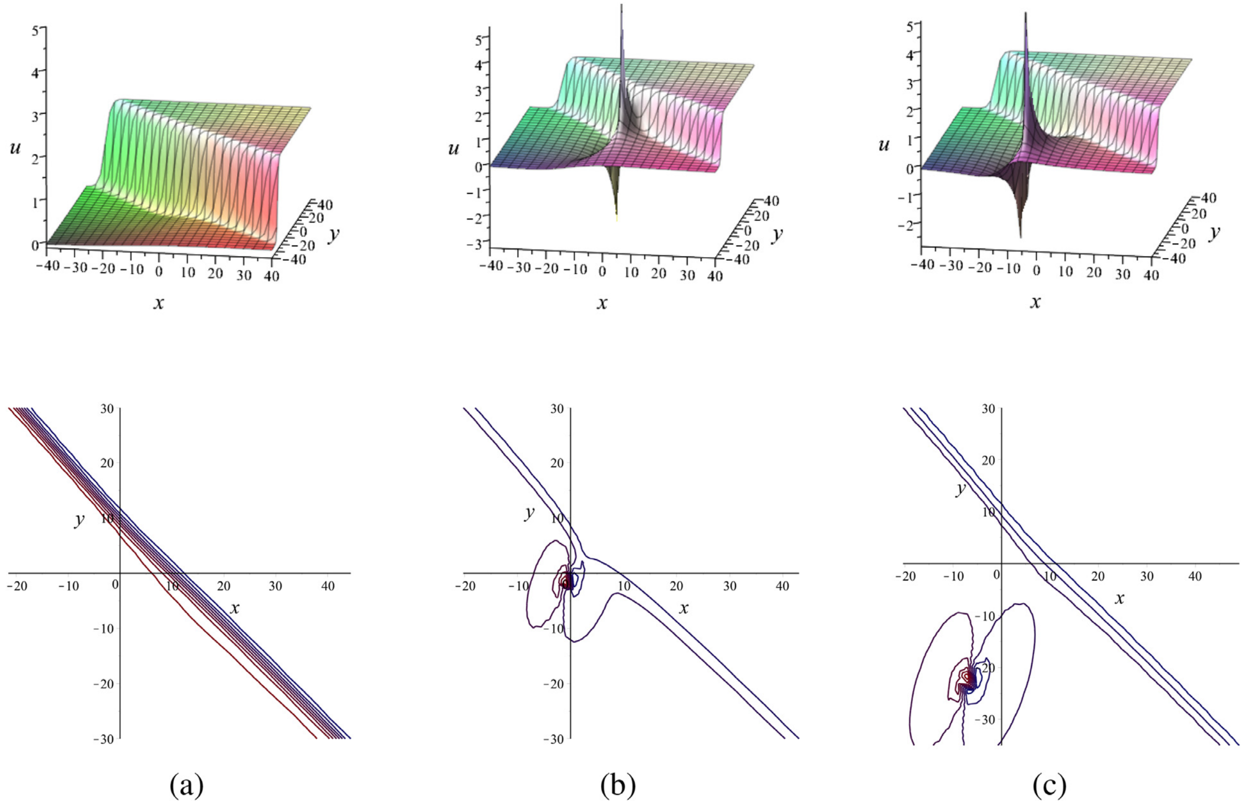

Fig. 3. Plots of interaction phenomena between a lump wave and a kink wave for $z = 1$ at times (a) $t = -40$, (b) $t = 1$, (c) $t = 18$.

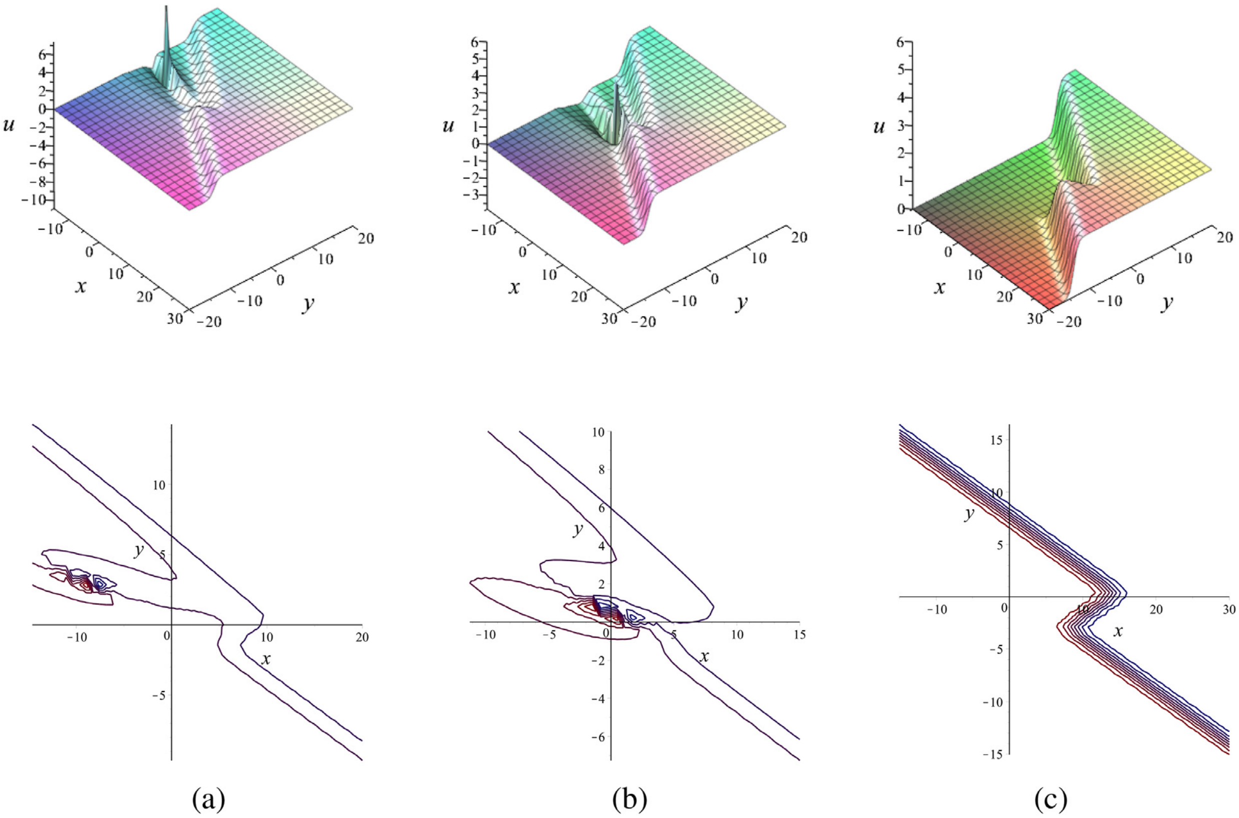

Fig. 4. Plots of interaction phenomena between a lump wave and a kink wave for $z = -1$ at times (a) $t = -1$, (b) $t = 0$, (c) $t = 30$.

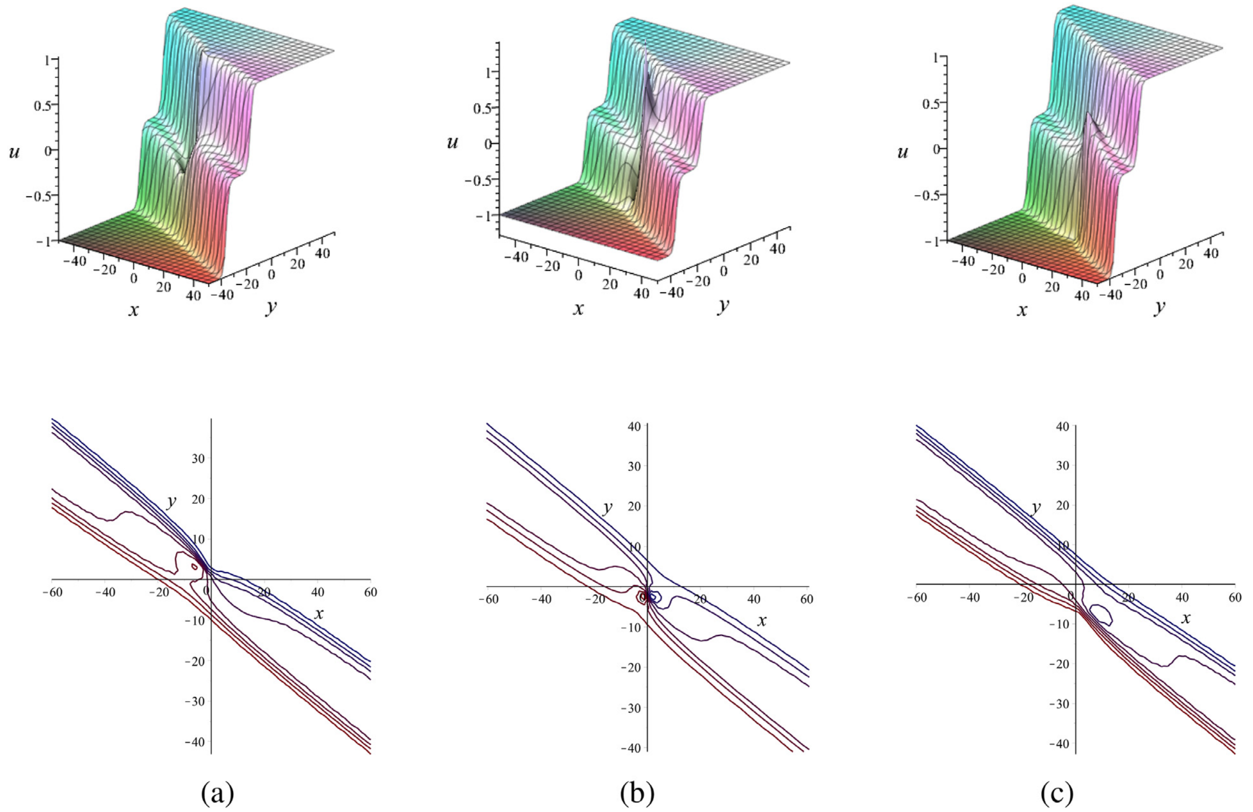

Fig. 5. Plots of interaction phenomena between a lump wave and two-kink waves for $z = 1$ at times (a) $t = -9$, (b) $t = 0$, (c) $t = 9$.

4. Interaction phenomena between a lump wave and multi-kink waves

To obtain interaction solutions between a lump wave and multi-kink waves to the (3+1)-dimensional HSII equation, we suppose that f is expressed in the following form

$$f = n_1^2 + n_2^2 + \sum_{i=1}^{N} \cosh(m_i) + c, \tag{26}$$

where

$$n_1 = a_1 x + a_2 y + a_3 z + a_4 t + a_5,$$
$$n_2 = a_6 x + a_7 y + a_8 z + a_9 t + a_{10},$$
$$m_i = b_{i1} x + b_{i2} y + b_{i3} z + b_{i4} t + b_{i5},$$

while $a_j \, (1 \le j \le 10), b_{i1}, b_{i2}, b_{i3}, b_{i4}, b_{i5} \, (1 \le i \le N)$ and c are all constants to be determined later.

Case 1

When $N = 1,\ u = 2(\ln f)_x$ degenerates into the interaction solution between a lump wave and two-kink waves. Substituting Eq. (26) into Eq. (7), and setting all the coefficients of x, y, z, t and $\cosh(m_i)$ to zero, we obtain two cases of solutions in Appendix B. A suitable set of parameters $\alpha = 1,\ \beta = -1,\ a_2 = 1,\ a_4 = 1,\ a_5 = 2,\ a_6 = 1,\ a_7 = \frac{3}{2},\ a_9 = 1,\ a_{10} = 2,\ b_{11} = \frac{1}{2},\ b_{12} = 1,\ b_{15} = \frac{1}{3}$ and $c = 2$ of the first case in Appendix B leads to

$$f = (-x + y + z + t + 2)^2 + \left(x + \frac{3}{2}y + \frac{3}{2}z + t + 2\right)^2 + \cosh\left(\frac{1}{2}x + y + \frac{9}{8}z + \frac{1}{3}\right) + 2, \tag{27}$$

and

$$\begin{aligned} u &= 2(\ln f(x, y, z, t))_x \\ &= \frac{2(4x + y + z + \frac{1}{2}\sinh(\frac{1}{2}x + y + \frac{9}{8}z + \frac{1}{3}))}{(-x + y + z + t + 2)^2 + (x + \frac{3}{2}y + \frac{3}{2}z + t + 2)^2 + \cosh(\frac{1}{2}x + y + \frac{9}{8}z + \frac{1}{3}) + 2}. \end{aligned} \tag{28}$$

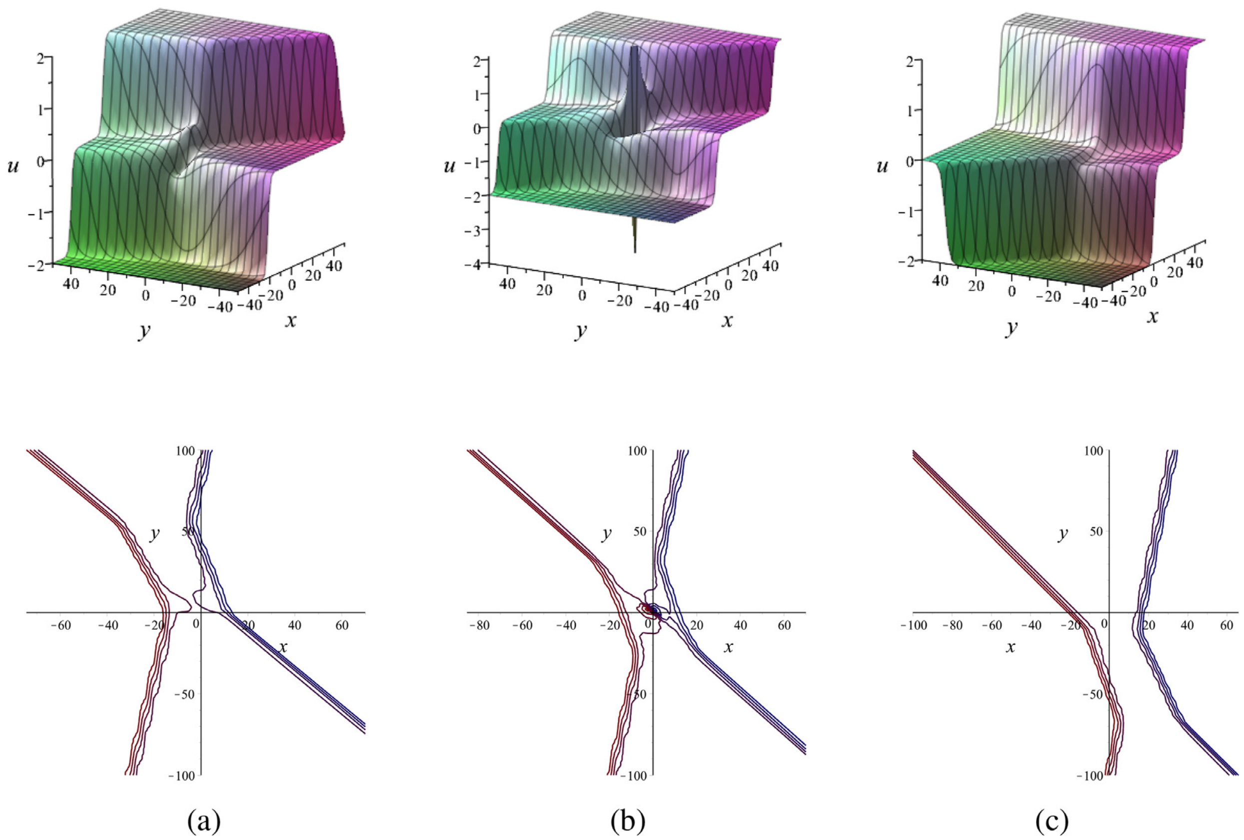

Fig. 6. Plots of interaction phenomena between a lump wave and two-kink waves for $z = 1$ at times (a) $t = -10$, (b) $t = 1$, (c) $t = 20$.

For further simulating the propagation of the lump wave, we assume

$$f_2 = 3 + (t - x + y + 3)^2 + \left(t + x + \frac{3}{2}y + \frac{7}{2}\right)^2. \tag{29}$$

Substituting the extreme point of $u_2 = 2(\ln f_2(x, y, t))_x$ into Eq. (28) with $z = 1$, we have

$$u = \frac{2\left(2\sqrt{6} - \frac{1}{2}\sinh\left(\frac{7}{10}t + \frac{113}{120} - \frac{\sqrt{6}}{4}\right)\right)}{5 + \cosh\left(\frac{7}{10}t + \frac{113}{120} - \frac{\sqrt{6}}{4}\right)}, \tag{30}$$

which represents the amplitude of the extreme point of u_2.

In Fig. 5, the two kink waves are parallel and remain unchanged in location. The lump wave generates from one of the kink waves and moves toward the other. Finally, the lump wave is gradually drowned or swallowed by the kink wave. Fig. 2(b) shows the amplitude of the extreme point of u_2. Since $\lim_{t\to-\infty} u = -1$ and $\lim_{t\to+\infty} u = 1$, the results illustrate that the lump wave can only move between two kink waves. The collision between a lump wave and two-kink waves is completely non-elastic.

Case 2

When $N = 2$, $u = 2(\ln f)_x$ degenerates into the interaction solution between a lump wave and two-kink waves. With symbolic computation, when $b_{14} = 1$, we obtain four cases of solutions in Appendix C. For a set of parameters $\alpha = -1$, $\beta = -2$, $c = 1$, $a_1 = 30$, $a_2 = 20$, $a_5 = 2$, $a_7 = -20$, $a_9 = 1$, $a_{10} = 2$, $b_{12} = \frac{1}{2}$, $b_{15} = -2$, $b_{21} = 1$, $b_{22} = \frac{1}{3}$ and $b_{25} = 1$ of the first case in Appendix C, we have

$$f = (30x + 20y - 10z + 2)^2 + (-20y + 10z + t + 2)^2 + 1 + \cosh\left(x + \frac{1}{3}y + \frac{1}{3}z + 1\right) + \cosh\left(\frac{1}{2}y - \frac{1}{4}z + t - 2\right), \tag{31}$$

and

$$u = 2(\ln f(x, y, z, t))_x = \frac{2(1800x + 1200y - 600z + 120 + \sinh(x + \frac{1}{3}y + \frac{1}{3}z + 1))}{f}. \tag{32}$$

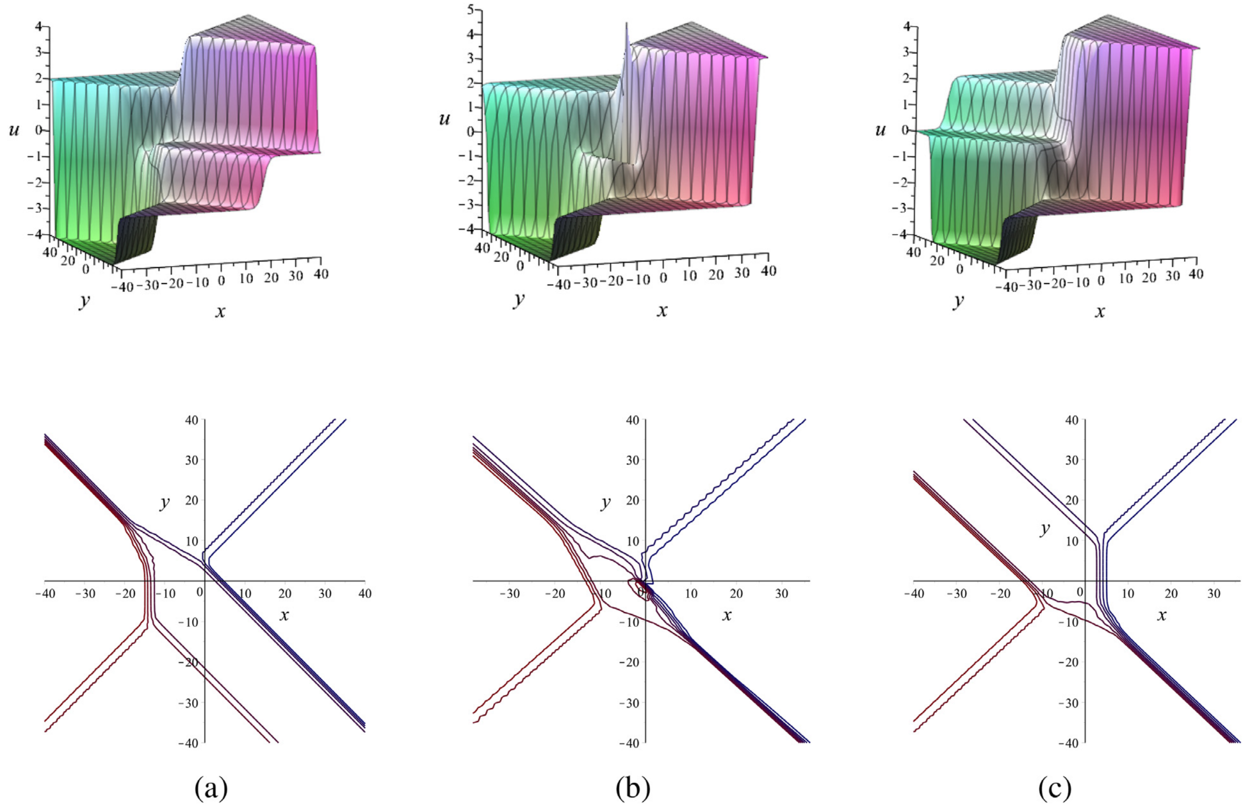

Fig. 7. Plots of interaction phenomena between a lump wave and three-kink waves for $z = 1$ at times (a) $t = -20$, (b) $t = 0$, (c) $t = 16$.

In Fig. 6, there exist two crossed kinks. Unlike the mechanism of interaction in Fig. 5, the lump wave generates from the intersection of two kink waves. From the dynamic property of the lump wave, it vanishes rapidly and the amplitude changes greatly, which conforms to the properties of the rogue wave. This progress illustrates the appearance of a kind of the rogue wave based on the interaction between lump wave and kink waves.

Case 3

When $N = 3,\ u = 2(\ln f)_x$ degenerates into the interaction solution between a lump wave and three-kink waves. We consider the case of $b_{24} = 1$ and derive three cases of parameters in Appendix D. When we choose $\alpha = 1,\ \beta = -1,\ c = 1,\ a_2 = 100,\ a_4 = -1,\ a_5 = 90,\ a_7 = 14,\ a_9 = 1,\ a_{10} = 2,\ b_{11} = 1,\ b_{12} = 2,\ b_{15} = 2,\ b_{22} = 1,\ b_{25} = 1,\ b_{31} = 2,\ b_{32} = 1$ and $b_{35} = 1$ of the first case, the solution of Eq. (7) is changed into

$$\begin{aligned} f =&(80x + 100y + 100z - t + 90)^2 + (80x + 14y + 14z + t + 2)^2 + \cosh(x + 2y + 3z + 2) \\ &+ \cosh(y + z + t + 1) + \cosh(2x + y + 9z + 1) + 1, \end{aligned} \tag{33}$$

and the solution to the (3+1)-dimensional HSI equation is

$$\begin{aligned} u &= 2(\ln f(x, y, z, t))_x \\ &= \frac{2(25600x + 18240y + 18240z + 14720 + \sinh(x + 2y + 3z + 2) + 2\sinh(2x + y + 9z + 1))}{f}. \end{aligned} \tag{34}$$

In Fig. 7, only one of the existing three kink waves maintains the position. Fig. 7(a)–(c) show two moving kink waves merge into a line in the second quadrant, both second and fourth quadrants, the fourth quadrant, respectively. The lump wave generates from the intersection of the kink waves. Finally, the lump wave is gradually drowned or swallowed by the kink waves.

5. Conclusions

In this paper, Bäcklund transformation of the (3+1)-dimensional HSI equation has been derived. We have constructed exponential function solutions from the known ones by applying the corresponding bilinear Bäcklund transformation. The test function method provides us with an efficient and direct method to solve NLEEs. Based on two test functions, including rational-multi-exp and rational-multi-cosh type test functions, we have discussed the interaction phenomena between the lump wave and multi-kink waves. Fig. 3 show that the lump wave generates from the kink wave and then separates from it. By contrast, the lump wave generates and gradually approaches the turning point of the kink wave, and finally the lump wave is swallowed by the kink wave in Fig. 4. Fig. 2(b) shows the amplitude of the extreme point of u_2. Since $\lim_{t\to-\infty} u = -1$ and $\lim_{t\to+\infty} u = 1$, the results illustrate that the lump wave can only move between two kink waves in Fig. 5. Moreover, the lump may occur in different positions. In Figs. 6 and 7, the lump wave generates from the intersection of kink waves. Especially, two moving kink waves merge into a line in different quadrants over time in Fig. 7. The diverse interaction phenomena might have great significance for the nonlinear waves in fluid mechanics. In the future, we aim to construct exact solutions based on some new Bäcklund transformations. The interaction between multi-lump and other solutions of NLEEs will also be further investigated. It is particularly pointed out that solving variable-coefficient equations is of great significance.

Declaration of Competing Interest

The authors declare that they have no known competing financial interests or personal relationships that could have appeared to influence the work reported in this paper.

Acknowledgments

This work is supported by the Fundamental Research Funds for the Central Universities of China (2018RC031), and the National Natural Science Foundation of China under Grant No. 71971015.

Appendix A

Case 1

$$\left\{a_1 = -\frac{a_6 a_9}{a_4},\ a_3 = -\frac{\alpha a_2}{\beta},\ a_5 = -\frac{a_9 a_{10}}{a_4},\ a_7 = -\frac{\beta a_8}{\alpha},\ k_3 = -\frac{k_1^3 + \alpha k_2}{\beta},\ k_4 = 0,\ k_5 = 0, k_7 = -\frac{\alpha k_6}{\beta},\ k_8 = 0\right\}.$$

Case 2

$$\left\{a_1 = -\frac{a_6 a_9}{a_4},\ a_3 = -\frac{\alpha a_2}{\beta},\ a_5 = 0,\ a_8 = -\frac{\alpha a_7}{\beta},\ a_{10} = 0,\ k_3 = -\frac{k_1^3 + \alpha k_2}{\beta},\ k_4 = 0,\ k_5 = -k_1, k_7 = -\frac{-k_1^3 + \alpha k_6}{\beta},\ k_8 = 0\right\}.$$

Appendix B

Case 1

$$\left\{a_1 = -\frac{a_6 a_9}{a_4}, a_3 = -\frac{\alpha a_2}{\beta}, a_8 = -\frac{\alpha a_7}{\beta}, b_{13} = -\frac{b_{11}^3 + \alpha b_{12}}{\beta}, b_{14} = 0\right\}. \tag{35}$$

Case 2

$$\left\{\alpha = -\frac{\beta a_8}{a_7}, a_2 = \frac{a_3 a_7}{a_8}, a_4 = 0, a_6 = 0, b_{12} = \frac{a_7(b_{11}^3 + \beta b_{13})}{\beta a_8}, b_{14} = 0\right\}. \tag{36}$$

Appendix C

Case 1

$$\left\{a_3 = -\frac{\alpha a_2}{\beta}, a_4 = 0, a_6 = 0, a_8 = -\frac{\alpha a_7}{\beta}, b_{11} = 0, b_{13} = -\frac{\alpha b_{12}}{\beta}, b_{23} = -\frac{b_{21}^3 + \alpha b_{22}}{\beta}, b_{24} = 0\right\}. \tag{37}$$

Case 2

$$\left\{\alpha = -\frac{\beta a_8}{a_7}, a_1 = -\frac{a_6 a_9}{a_4}, a_2 = 0, a_3 = 0, b_{11} = 0, b_{13} = \frac{a_8 b_{12}}{a_7}, b_{23} = \frac{-b_{21}^3 a_7 + \beta b_{22} a_8}{\beta a_7}, b_{24} = 0\right\}. \tag{38}$$

Case 3

$$\left\{a_1 = -\frac{a_6 a_9}{a_4}, a_3 = -\frac{\alpha a_2}{\beta}, a_8 = -\frac{\alpha a_7}{\beta}, b_{11} = 0, b_{13} = -\frac{\alpha b_{12}}{\beta}, b_{23} = -\frac{b_{21}^3 + \alpha b_{22}}{\beta}, b_{24} = 0\right\}. \tag{39}$$

Case 4

$$\left\{a_3 = -\frac{\alpha a_2}{\beta}, a_4 = -\frac{a_7 a_9}{a_2}, a_6 = \frac{a_1 a_7}{a_2}, a_8 = -\frac{\alpha a_7}{\beta}, a_{10} = \frac{a_5 a_7}{a_2}, b_{11} = 0, b_{13} = -\frac{\alpha b_{12}}{\beta}, b_{23} = -\frac{b_{21}^3 + \alpha b_{22}}{\beta}, b_{24} = 0\right\}. \tag{40}$$

Appendix D

Case 1

$$\left\{a_1=-\frac{a_6a_9}{a_4},a_3=-\frac{\alpha a_2}{\beta},a_8=-\frac{\alpha a_7}{\beta},b_{13}=-\frac{b_{11}^3+\alpha b_{12}}{\beta},b_{14}=0,b_{21}=0,b_{23}=-\frac{\alpha b_{22}}{\beta},b_{33}=-\frac{b_{31}^3+\alpha b_{32}}{\beta},b_{34}=0\right\}. \tag{41}$$

Case 2

$$\left\{\alpha=-\frac{\beta a_8}{a_7},a_1=-\frac{a_6a_9}{a_4},a_2=0,a_3=0,b_{13}=\frac{-a_7b_{11}^3+\beta a_8b_{12}}{\beta a_7},b_{14}=0,b_{21}=0,b_{23}=\frac{a_8b_{22}}{a_7},\right.$$
$$\left.b_{33}=\frac{-a_7b_{31}^3+\beta a_8b_{32}}{\beta a_7},b_{34}=0\right\}. \tag{42}$$

Case 3

$$\left\{a_3=-\frac{\alpha a_2}{\beta},a_4=-\frac{a_7a_9}{a_2},a_6=\frac{a_1a_7}{a_2},a_8=-\frac{\alpha a_7}{\beta},a_{10}=\frac{a_5a_7}{a_2},b_{13}=-\frac{b_{11}^3+\alpha b_{12}}{\beta},b_{14}=0,\right.$$
$$\left.b_{21}=0,b_{23}=-\frac{\alpha b_{22}}{\beta},b_{33}=-\frac{b_{31}^3+\alpha b_{32}}{\beta},b_{34}=0\right\}. \tag{43}$$

References

[1] Ablowitz MJ, Kaup DJ, Newell AC, Segur H. Nonlinear-evolution equations of physical significance. Phys Rev Lett 1973;31(2):125–7.
[2] He J, Abdou M. New periodic solutions for nonlinear evolution equations using exp-function method. Chaos Solitons Fract 2007;34(5):1421–9.
[3] Abdou MA. The extended f-expansion method and its application for a class of nonlinear evolution equations. Chaos Solitons Fract 2007;31(1):95–104.
[4] Fan EG. Multiple travelling wave solutions of nonlinear evolution equations using a unified algebraic method. J Phys A: Math Gen 2002;35(32):6853–72.
[5] Xie JJ, Yang X. Rogue waves, breather waves and solitary waves for a (3+1)-dimensional nonlinear evolution equation. Appl Math Lett 2019;97:6–13.
[6] Chen SJ, Yin YH, Ma WX, Lü X. Abundant exact solutions and interaction phenomena of the (2+1)-dimensional YTSF equation. Analy Math Phys 2019;9:2329–44.
[7] Lü X, Lin FH, Qi FH. Analytical study on a two-dimensional Korteweg-de Vries model with bilinear representation, Bäcklund transformation and soliton solutions. Appl Math Model 2015;39:3221–6.
[8] Gao LN, Zhao XY, Zi YY, Yu J, Lü X. Resonant behavior of multiple wave solutions to a Hirota bilinear equation. Comput Math Applica 2016;72:1225–9.
[9] Xu HN, Ruan WY, Zhang Y, Lü X. Multi-exponential wave solutions to two extended Jimbo-Miwa equations and the resonance behavior. Appl Math Lett 2020;99:105976.
[10] Hua YF, Guo BL, Ma WX, Lü X. Interaction behavior associated with a generalized (2 + 1)-dimensional Hirota bilinear equation for nonlinear waves. Appl Math Model 2019;74:184–98.
[11] Lü X, Ma WX, Yu J, Lin F, Khalique CM. Envelope bright- and dark-soliton solutions for the Gerdjikov-Ivanov model. Nonlinear Dyn 2015;82(3):1–10.
[12] Lü X, Chen ST, Ma WX. Constructing lump solutions to a generalized Kadomtsev-Petviashvili-Boussinesq equation. Nonlinear Dyn 2016;86(1):523–34.
[13] Lü X, Ma WX. Study of lump dynamics based on a dimensionally reduced Hirota bilinear equation. Nonlinear Dyn 2016;85(2):1–6.
[14] Kurt A, Tasbozan O. Analytic solutions of Liouville equation using extended trial equation method and the functional varible method. Appl Math Inform Sci Lett 2015;3(3):93–6.
[15] Osman MS. New analytical study of water waves described by coupled fractional variant Boussinesq equation in fluid dynamics. Pramana 2019;93(2):26.
[16] Osman MS, Ghanbari B. New optical solitary wave solutions of Fokas-Lenells equation in presence of perturbation terms by a novel approach. Optik 2018;175:328–33.
[17] Levi D, Benguria R. Bäcklund transformations and nonlinear differential difference equations. Proc Natl Acad Sci USA 1980;77:5025–7.
[18] Cheng JP, He JS. Miura and auto-Bäcklund transformations for the discrete KP and mKP hierarchies and their constrained cases. Commun Nonlinear Sci Num Simul 2019;69:187–97.
[19] Hirota R. The Direct Method in Soliton Theory. Cambridge University Press; 2004.
[20] Rogers C, Shadwick WF. Bäcklund Transformations and Their Applications. Academic Press; 1982.
[21] Yin YH, Ma WX, Liu JG, Lü X. Diversity of exact solutions to a (3+1)-dimensional nonlinear evolution equation and its reduction. Comput Math Applica 2018;76:1275–83.
[22] Lü X, Zhu HW, Meng XH, Yang ZC, Tian B. Soliton solutions and a Bäcklund transformation for a generalized nonlinear Schrödinger equation with variable coefficients from optical fiber communications. J Math Analy Applica 2007;336(2):1305–15.
[23] Lü X, Tian B, Sun K, Wang P. Bell-polynomial manipulations on the Bäcklund transformations and Lax pairs for some soliton equations with one tau-function. J Math Phys 2010;51(11):113506.
[24] Zhao ZL. Bäcklund transformations, rational solutions and soliton-cnoidal wave solutions of the modified Kadomtsev-Petviashvili equation. Appl Math Lett 2019;89:103–10.
[25] Luo L. Bäcklund transformation of variable-coefficient Boiti-Leon-Manna-Pempinelli equation. Appl Math Lett 2019;94:94–8.
[26] Conte R, Musette M. Painlevé analysis and Bäcklund transformation in the Kuramoto-Sivashinsky equation. J Phys A: Math Gen 1989;22(2):169–77.
[27] Deng SF. Bäcklund transformation and soliton solutions for KP equation. Chaos Solitons Fract 2005;25(2):475–80.
[28] Ma WX, Abdeljabbar A. A bilinear Bäcklund transformation of a (3+1)-dimensional generalized KP equation. Appl Math Lett 2012;25:1500–4.
[29] Liu N. Bäcklund transformation and multi-soliton solutions for the (3+1)-dimensional BKP equation with Bell polynomials and symbolic computation. Nonlinear Dyn 2015;82(1–2):311–18.
[30] Ma WX. Lump solutions to the Kadomtsev-Petviashvili equation. Phys Lett A 2015;379(36):1975–8.
[31] He CH, Tang YN, Ma JL. New interaction solutions for the (3+1)-dimensional Jimbo-Miwa equation. Comput Math Applica 2018;76(9):2141–7.
[32] Lü X, Ma WX, Chen ST, Khalique CM. A note on rational solutions to a Hirota-Satsuma-like equation. Appl Math Lett 2016;58:13–18.
[33] Tang YN, Tao SQ, Zhou ML, Guan Q. Interaction solutions between lump and other solitons of two classes of nonlinear evolution equations. Nonlinear Dyn 2017;89(2):1–14.

[34] Lü X, Ma WX, Zhou Y, Khalique CM. Rational solutions to an extended Kadomtsev-Petviashvili-like equation with symbolic computation. Comput Math Applica 2016;71:1560–7.
[35] Wang CJ. Spatiotemporal deformation of lump solution to (2+1)-dimensional KdV equation. Nonlinear Dyn 2016;84(2):697–702.
[36] Sun HQ, Chen AH. Rational solutions and lump solutions of the potential YTSF equation. Zeitschrift für Naturforschung A 2017;72((7)a):665–72.
[37] Gao LN, Zi YY, Yin YH, Lü X. Bäcklund transformation, multiple wave solutions and lump solutions to a (3+1)-dimensional nonlinear evolution equation. Nonlinear Dyn 2017;89:2233.
[38] Zhao ZL, He LC. Multiple lump solutions of the (3+1)-dimensional potential Yu-Toda-Sasa-Fukuyama equation. Appl Math Lett 2019;95:114–21.
[39] Mironov VA, Smirnov AI, Smirnov LA. Structure of vortex shedding past potential barriers moving in a Bose-Einstein condensate. J Exper Theor Phys 2010;110(5):877–89.
[40] Falcon, éric, Laroche C, Fauve, Stéphan. Observation of depression solitary surface waves on a thin fluid layer. Phys Rev Lett 2002;89(20):204501.
[41] Singh N, Stepanyants Y. Obliquely propagating skew KP lumps. Wave Motion 2016;64:92–102.
[42] Lü X, Ma WX, Yu J. Khalique CM, Solitary waves with the Madelung fluid description: A generalized derivative nonlinear Schrödinger equation. Commun Nonlinear Sci Numer Simulat 2016;31:40–6.
[43] Hu YJ, Chen HL, Dai ZD. New kink multi-soliton solutions for the (3+1)-dimensional potential-Yu-Toda-Sasa-Fukuyama equation. Appl Math Comput 2014;234(C):548–56.
[44] Huang LL, Chen Y. Lump solutions and interaction phenomenon for (2+1)-dimensional Sawada-Kotera equation. Commun Theor Phys 2017;67(5):473–8.
[45] He CH, Tang YN, Ma WX, L MJ. Interaction phenomena between a lump and other multi-solitons for the (2+1)-dimensional BLMP and Ito equations. Nonlinear Dyn 2019;95:29–42.
[46] Lü X, Lin FH. Soliton excitations and shape-changing collisions in alphahelical proteins with interspine coupling at higher order. Commun Nonlinear Sci Numer Simulat 2016;32:241–61.
[47] Zhang XE, Chen Y, Tang XY. Rogue wave and a pair of resonance stripe solitons to KP equation. Comput Math Applica 2018;76:1938–49.
[48] Hirota R, Satsuma J. N-Soliton solutions of model equations for shallow water waves. J Phys Soc Jpn 1976;40(2):611–12.
[49] Zhou Y, Solomon M, Ma WX. Lump and lump-soliton solutions to the Hirota-Satsuma-Ito equation. Commun Nonlinear Sci Num Simul 2019;68:56–62.